Materials Informed Data Driven Design of Additive Structures (MID^{3}AS)

Paul Shade, Michael Groeber,
Edwin Schwalbach, Michael Uchic,
Bill Musinski, Sean Donegan, Daniel Sparkman,
TJ Turner, & Jonathan Miller
Air Force Research Laboratory
Materials & Manufacturing Directorate

Integrity ★ Service ★ Excellence

Integrated Computational Materials Engineering (ICME)

- Materials are heterogeneous
- Properties are function of chemistry and microstructure, which are a result of processing (strain, cooling rate, etc.)
- Smaller statistical distributions locally
- ICME – New paradigm for structural materials design

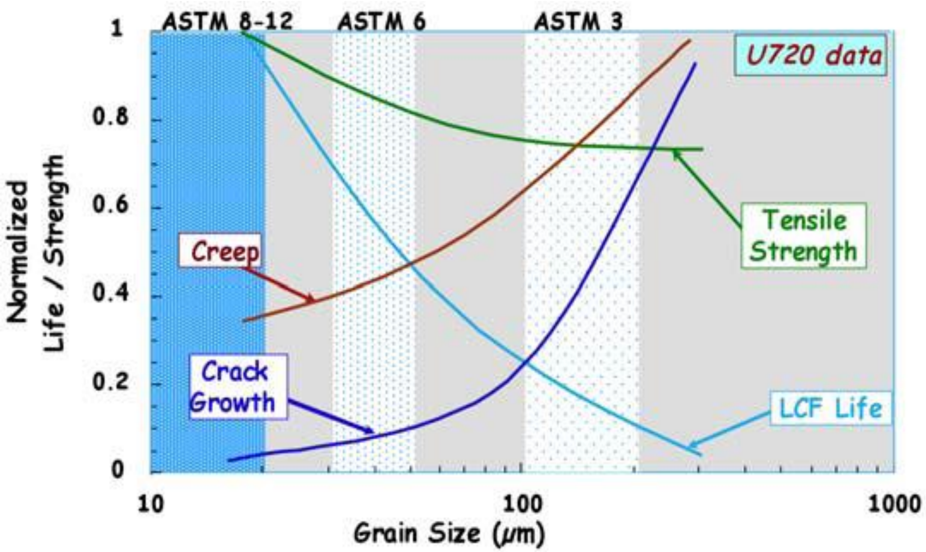

Adapted from J.C. Williams.

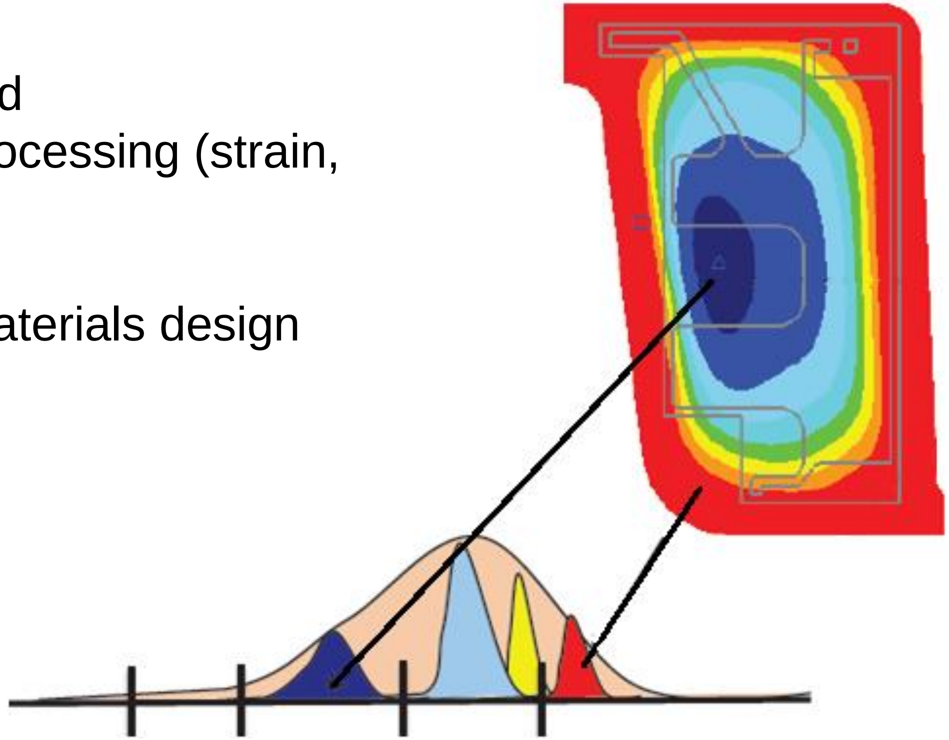

Adapted from D. Furrer, et al.

Goal: Develop and validate modeling capability to predict processing-structure-performance relationships

Local Processing Challenges: Additive Manufacturing

Void variability in laser processed Ti-6Al-4V

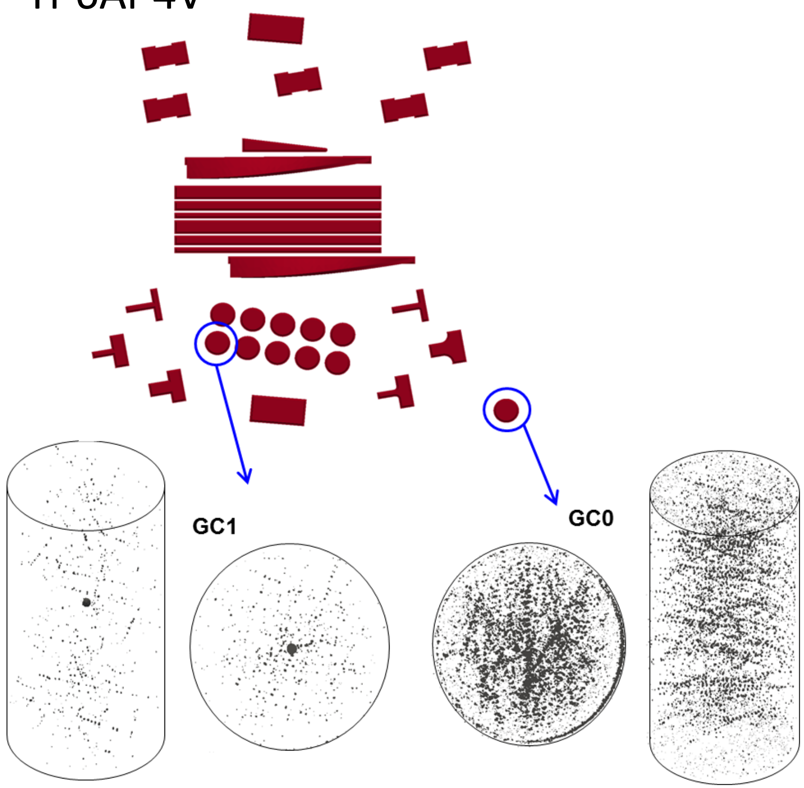

E Schwalbach, MA Groeber, J Miller

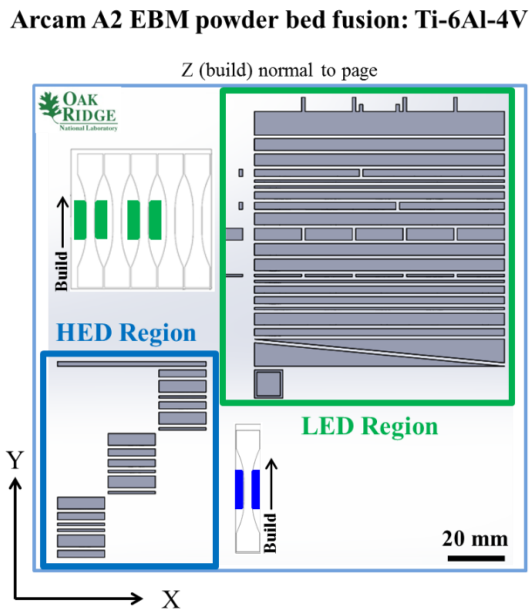

Oak Ridge National Lab

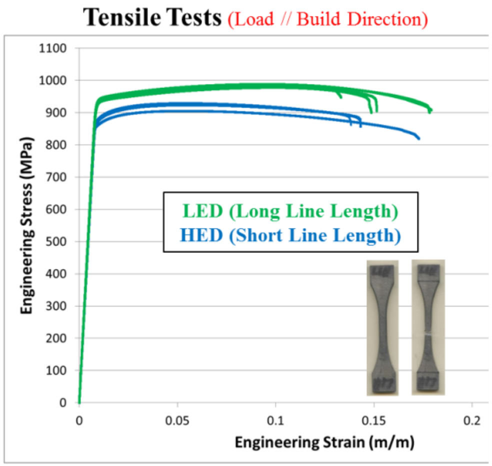

HED to LED Samples

- 10% Increase in YS, UTS
- Uniform strain and hardening
- Similar Ductility

Tensile variability (due to texture) in electron beam processed Ti-6Al-4V

Global processing variables are not sufficient to represent local processing – will drive 'variability'

Residual Stress in Additive Manufacturing

Residual stress in laser processed IN625
Measured with neutron diffraction

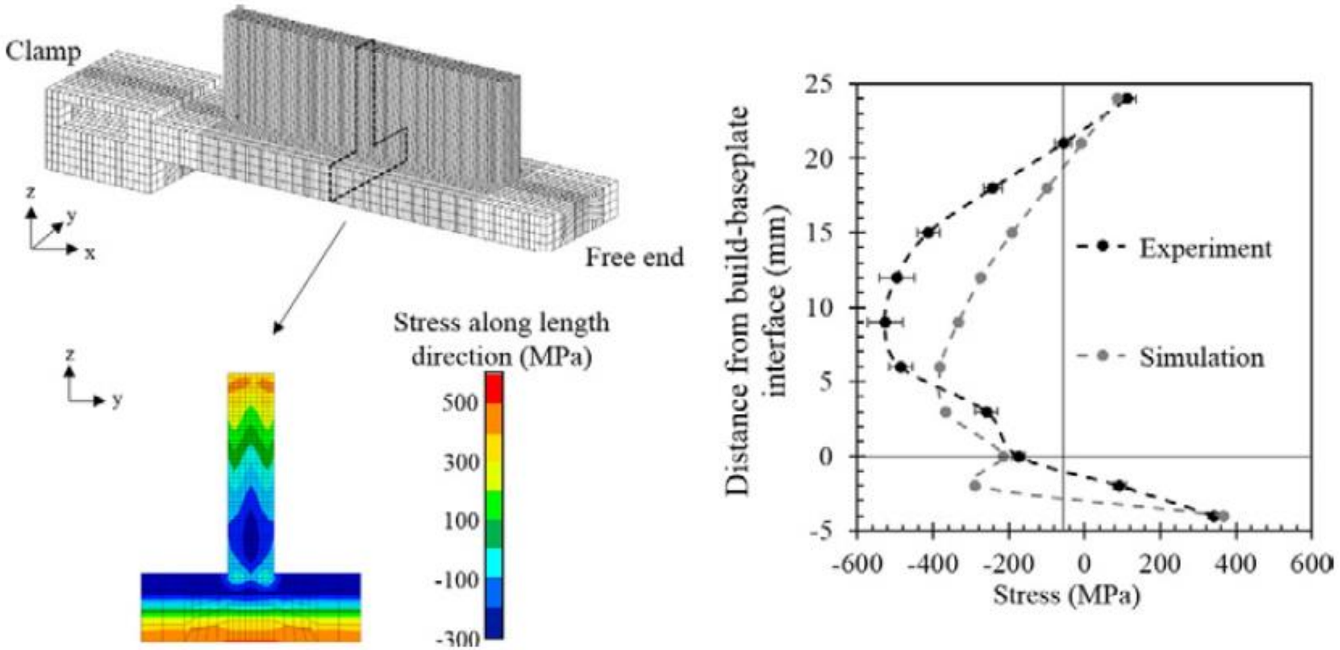

Wang Z, Denlinger E, Michaleris P, Stoica AD, Ma D, Beese AM. 2017. *Mater. Des.* 113:169-177

Rapid solidification and complex thermal histories
Leading to residual stress, geometrical distortion, damage, etc

Materials Informed Data Driven Design of Additive Structures (MID^{3}AS)

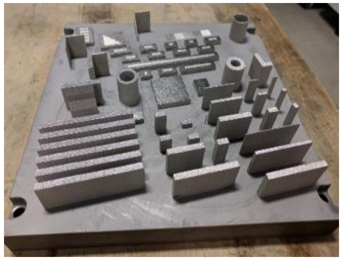

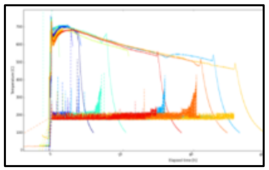

+

Microstructure - Texture

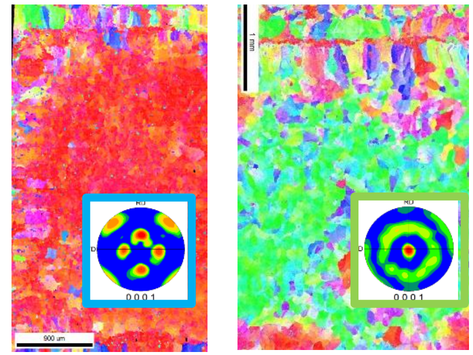

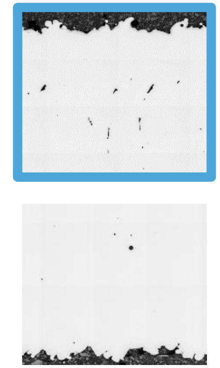

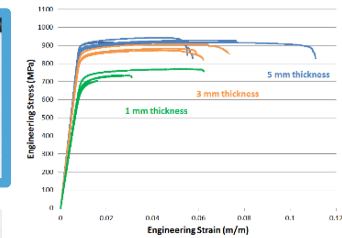

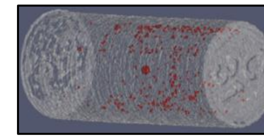

High-fidelity Detailed Processing, Structure & Property Characterization

Highly-Pedigreed AM Builds

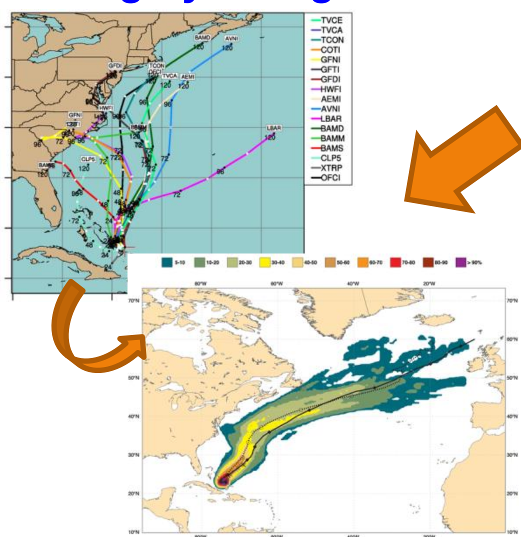

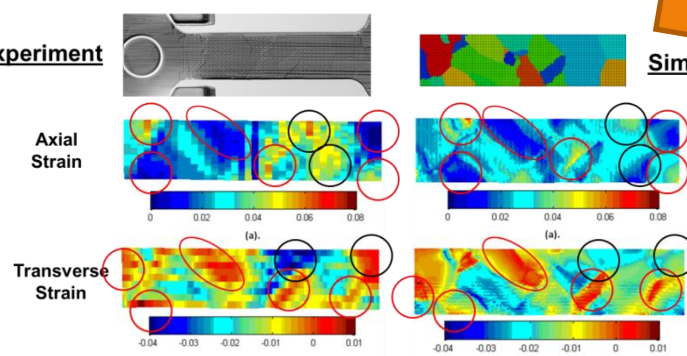

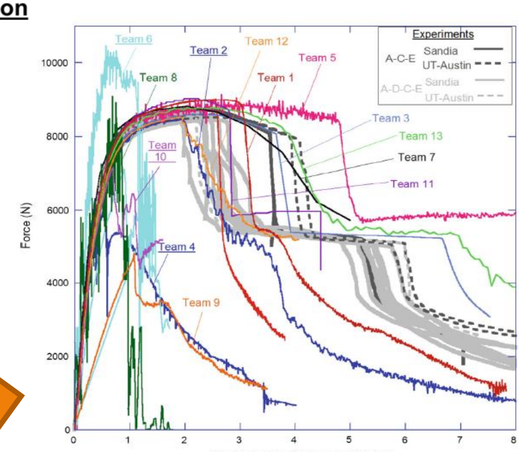

Validation & Benchmarking of Current Forecasts

Actionable Materials Forecasts

Community Challenges

MID^{3}AS Challenge Problems

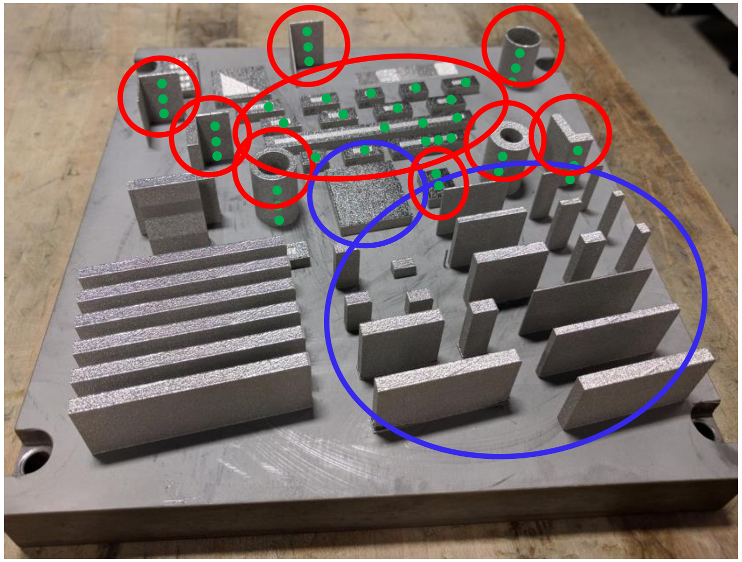

Process to Structure

Macro/Continuum Level

Calibration Data:

Residual stress & geometric distortions for 'thin walls' of multiple thicknesses & lengths

Input Data:

Build geometry, beam scan path, 3-5 locations of several sub-articles, powder morphology & chemistry, thermal & mechanical property references

Quantities to Forecast:

1) Residual stress @ 3-5 locations of several as-printed sub-articles
2) Geometric distortions of several as-printed sub-articles

Micro/Scan Path Level

Calibration Data:

Single bead geometry, grain size, defect morphology, texture for multiple power & speed combinations

Input Data:

Build geometry, beam scan path, powder morphology & chemistry, thermal properties

Quantities to Forecast:

1) As printed geometry of several '2D' objects
2) Grain size, defect morphology, texture @ 3-5 locations in several '2D' objects

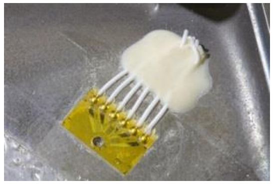

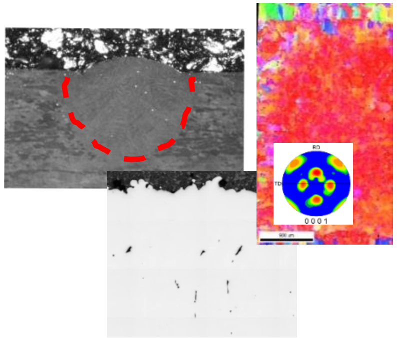

Simple geometries for known scan path and simulation feasibility

Preliminary Model Results

Results for quarter of plate

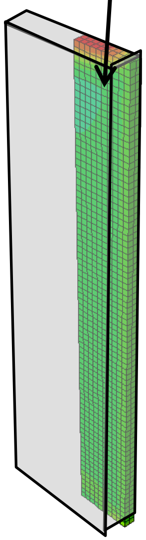

Lateral in-plane component

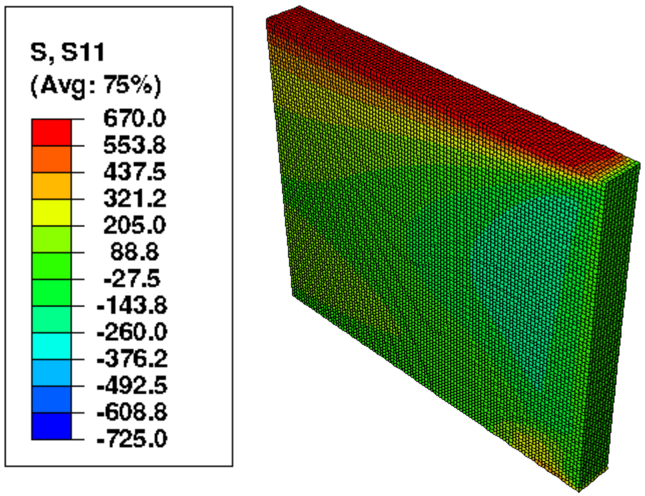

Vertical in-plane component

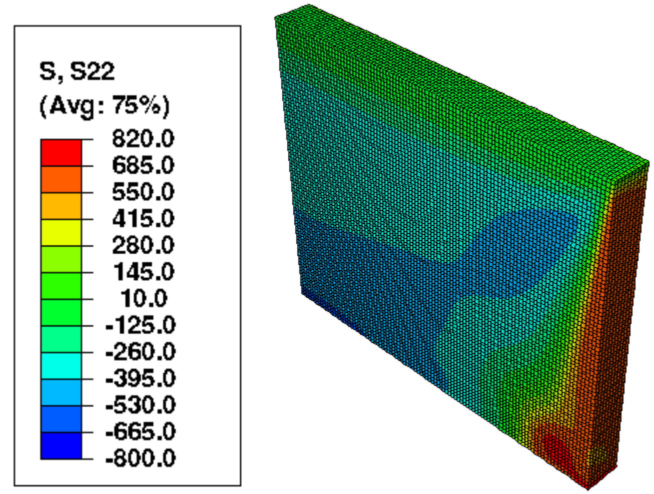

WD Musinski (AFRL)

- FEM simulations in ABAQUS
- Estimated thermal histories
- Temperature dependent properties: elastic modulus, yield strength, etc
- Structure built up ‘layer-by-layer’
- Parametric study of various build geometries – aid experimental design

Energy Dispersive Diffraction

Bragg's Law
$n\lambda = 2d \sin \theta$

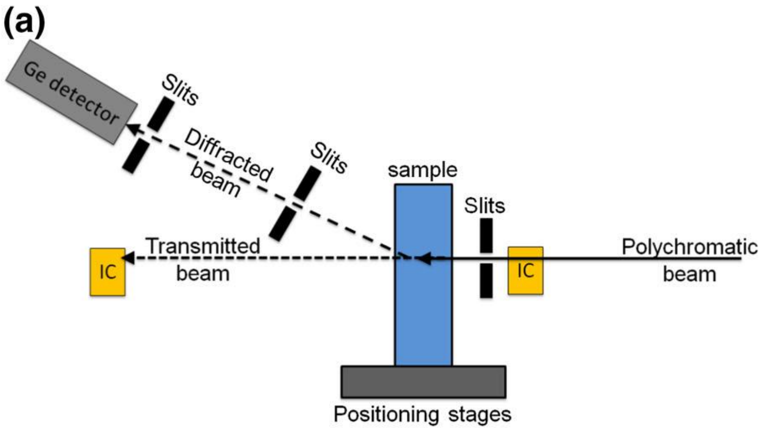

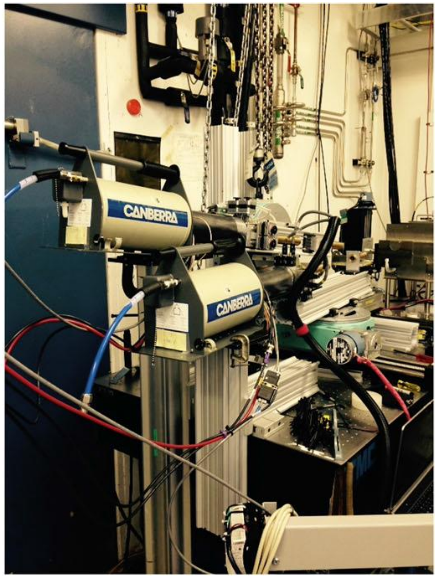

Mach JC, Budrow CJ, Pagan DC, Ruff JPC, Park J-S, Okasinski J, Beaudoin AJ, Miller MP. 2017. *JOM*

- Polychromatic (white) beam
- θ fixed, observe λ
  - Energy sensitive detector(s)
- Residual stress one of the main applications
- High flux enables measurement through relatively 'thick' (1-25 mm) samples
- Measurement time typically minutes/point
- Resolution may be as fine as ~20 μm orthogonal to beam, but 0.2-1 mm is more common
- Typical resolution along beam 1-5 mm

Preliminary Experimental Results

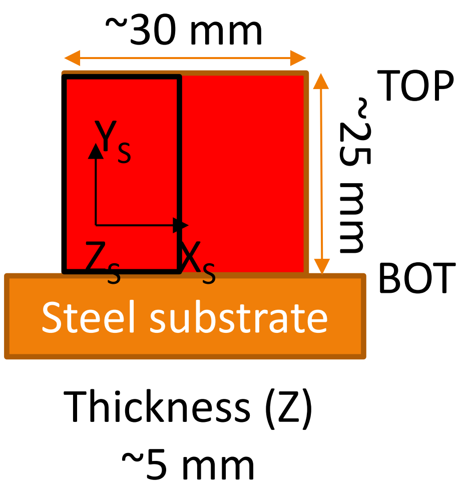

J-S Park, A Chuang
APS 6-BM

Lateral in-plane component

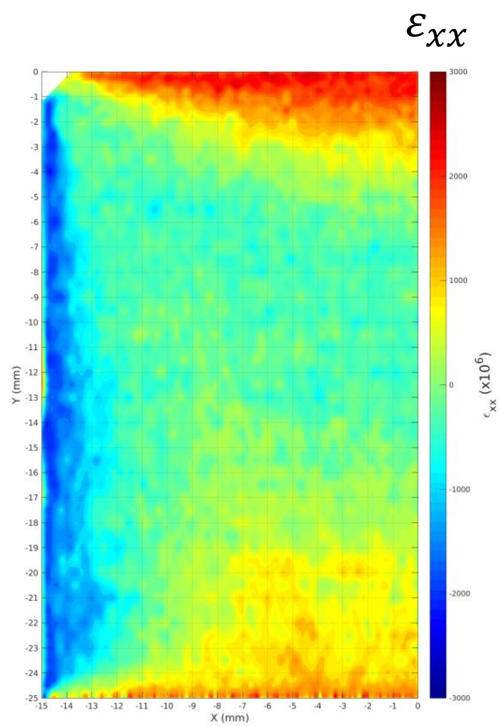

Vertical in-plane component

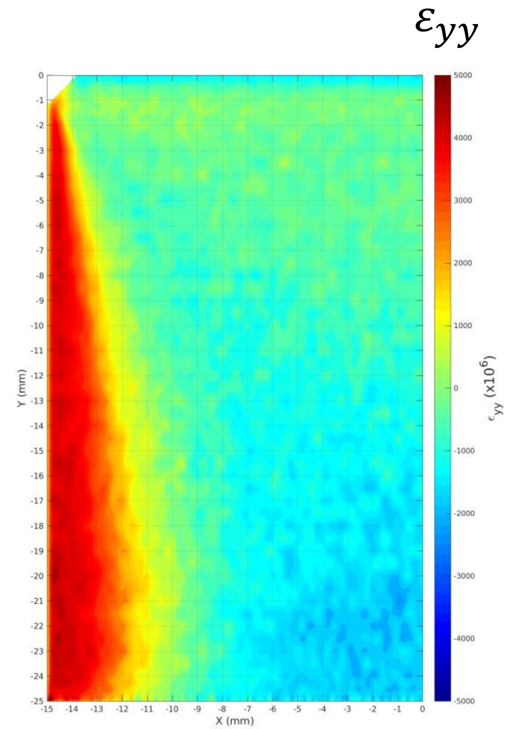

- Energy Dispersive X-ray Diffraction
- Reference lattice parameter measured on powder
- Coarse scan (0.5 mm) then fine scan (0.05 mm) across gradient regions
- Results shown are averages from {111}, {200}, {220}, and {311} peaks
- Trends in qualitative agreement with simulations

MID^{3}AS Challenge Problems

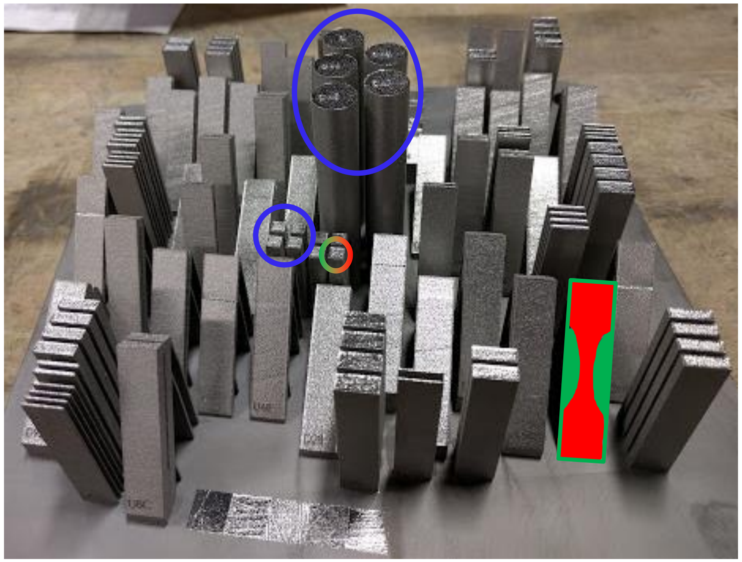

Structure to Properties

Continuum Level

Calibration Data:

ASTM E8 tests, grain & defect structure

Input Data:

Sample geometry, chemistry, grain size, texture, defect morphology, surface roughness, loading condition, environment

Quantities to Forecast:

1) Key values (E, σ_{YS}, m, σ_{UTS}, ε_{UE}, ε_F) on S-S curve (avg & std dev) for ground samples
2) Key values (E, σ_{YS}, m, σ_{UTS}, ε_{UE}, ε_F) on S-S curve (avg & std dev) for as-printed samples

Microstructure Level

Calibration Data:

ASTM E8 tests, Stress-strain curves for similar HEDM specimens (2-3)

Input Data:

Initial state of sample (near-field, far-field, tomography), elastic constants, chemistry

Quantities to Forecast:

1) Key values (E, σ_{YS}, m, σ_{UTS}, ε_{UE}, ε_F) on S-S curve
2) Stress evolution in ~10 grains
3) Location of damage localization

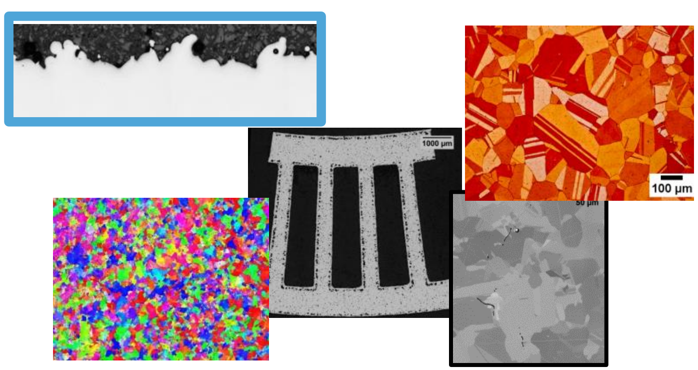

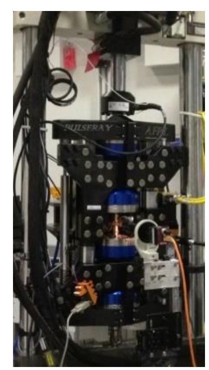

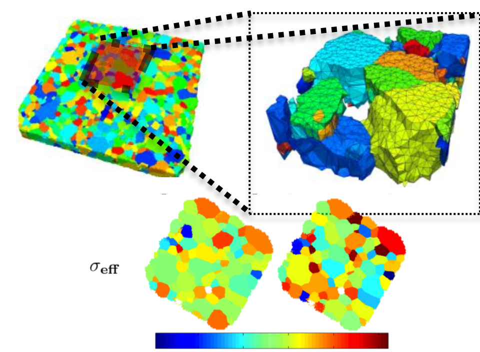

Relevant material using industry 'best practices', tests with variety of methods

Experimental Techniques

- ***Integration*** *of* three synchrotron x-ray techniques with ***in situ*** loading
- Micro-computed tomography (μ-CT)
  - Structure of voids/cracks

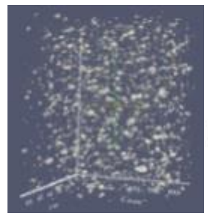

- Near field HEDM/3DXRD
  - 3D grain structure with sub-grain orientation resolution

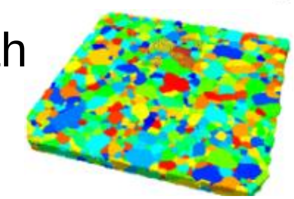

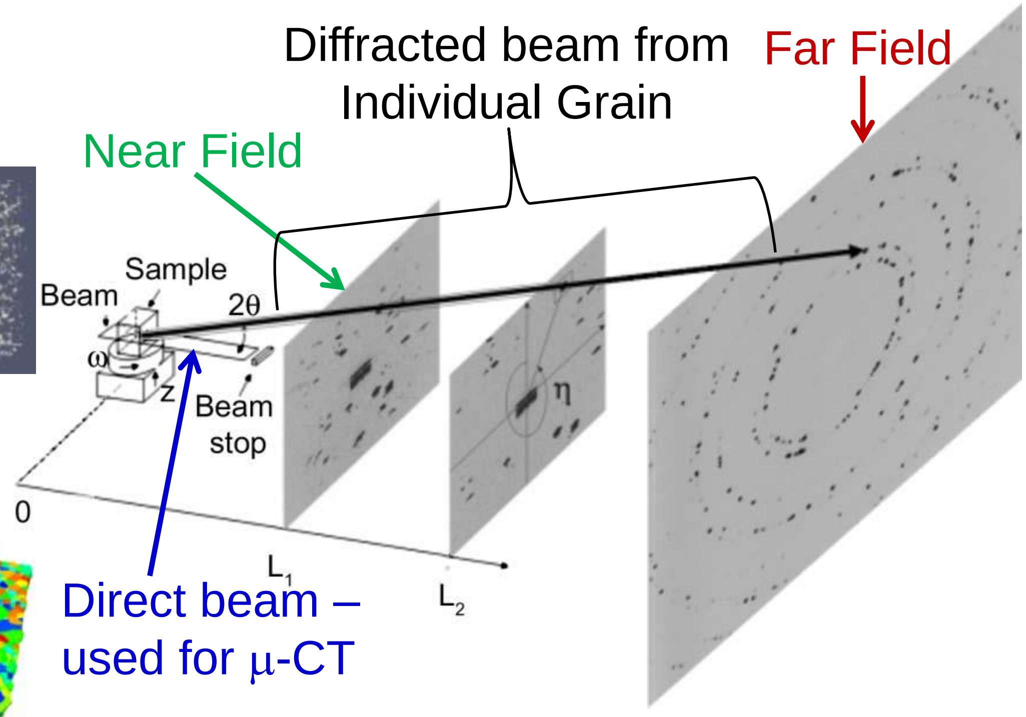

Adapted from: Poulsen HF. 2012. *J. Appl. Crystallogr.* 45:1084-1097

- Far field HEDM/3DXRD
  - Grain (or grain cross-section) resolved elastic strain tensors

$$\sigma_{ij} = C_{ijkl}\varepsilon_{kl}$$

Stress tensor with knowledge of elastic constants

RAMS Load Frame Insert

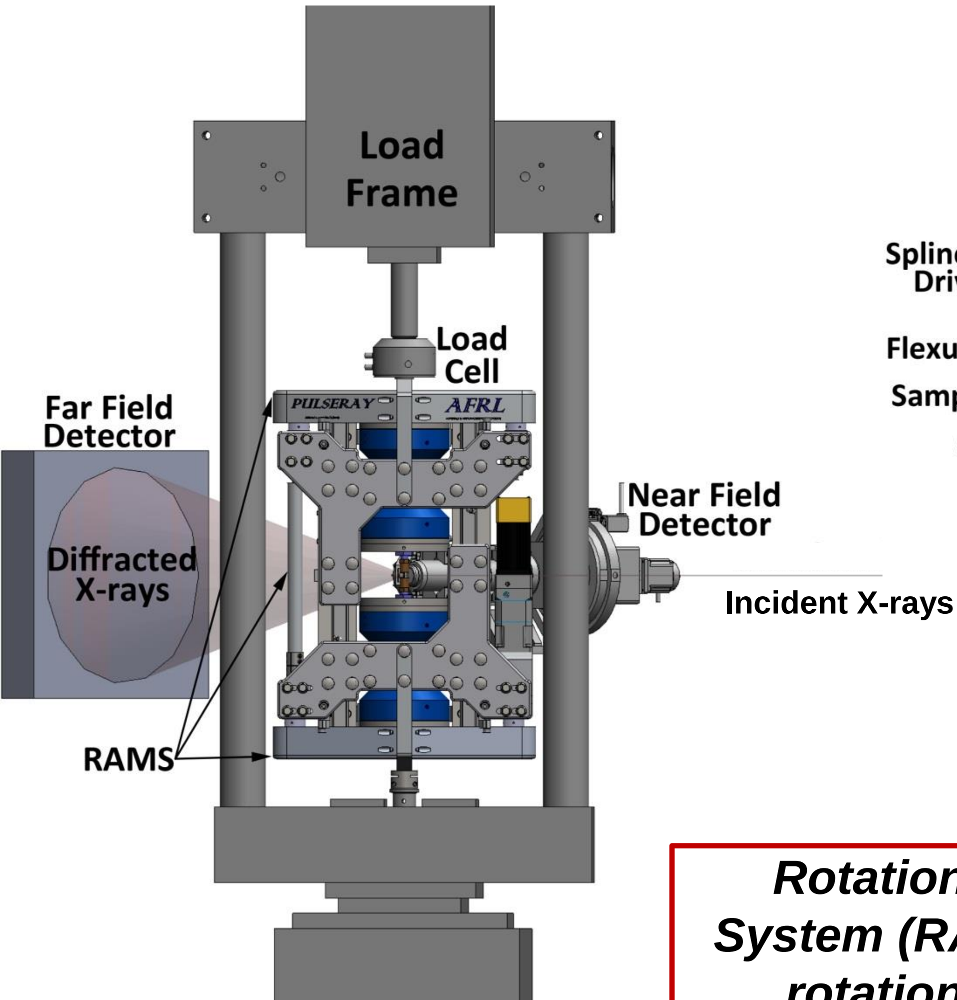

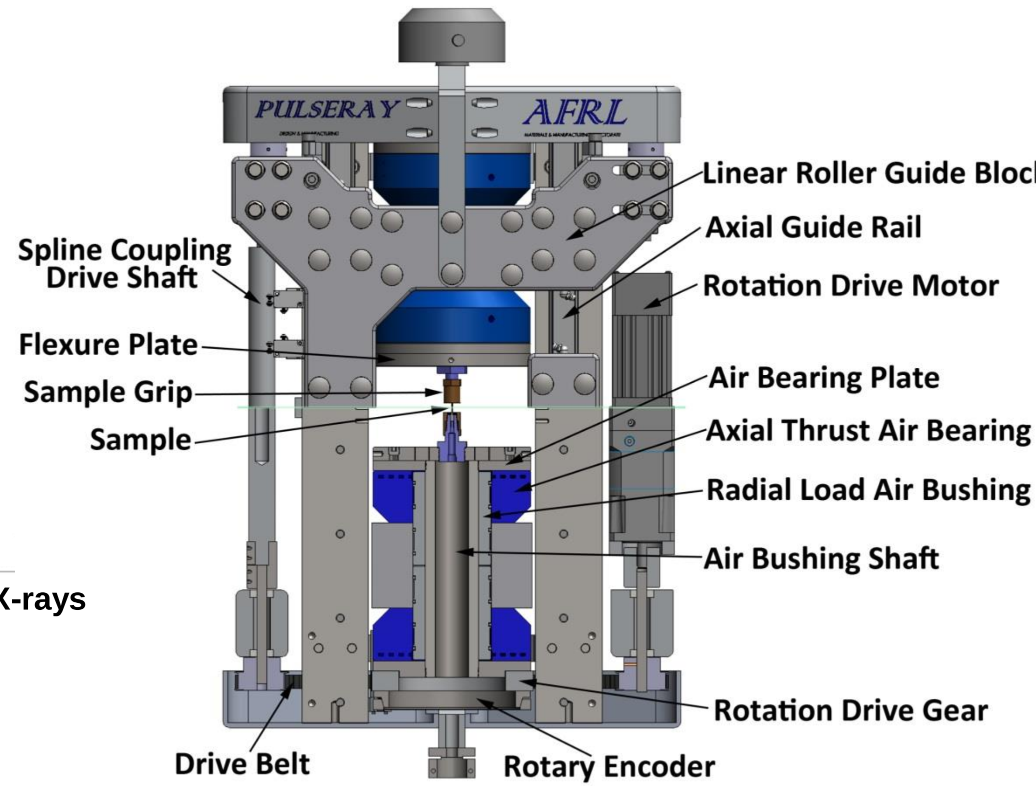

Rotational and Axial Motion System (RAMS): Enables sample rotation during concurrent tension/compression loading

Shade PA, Blank B, Schuren JC, Turner TJ, Kenesei P, Goetze K, Suter RM, Bernier JV, Li SF, Lind J, Lienert U, Almer J. 2015. *Rev. Sci. Instrum.* 86:093902

Grain Resolved Stresses

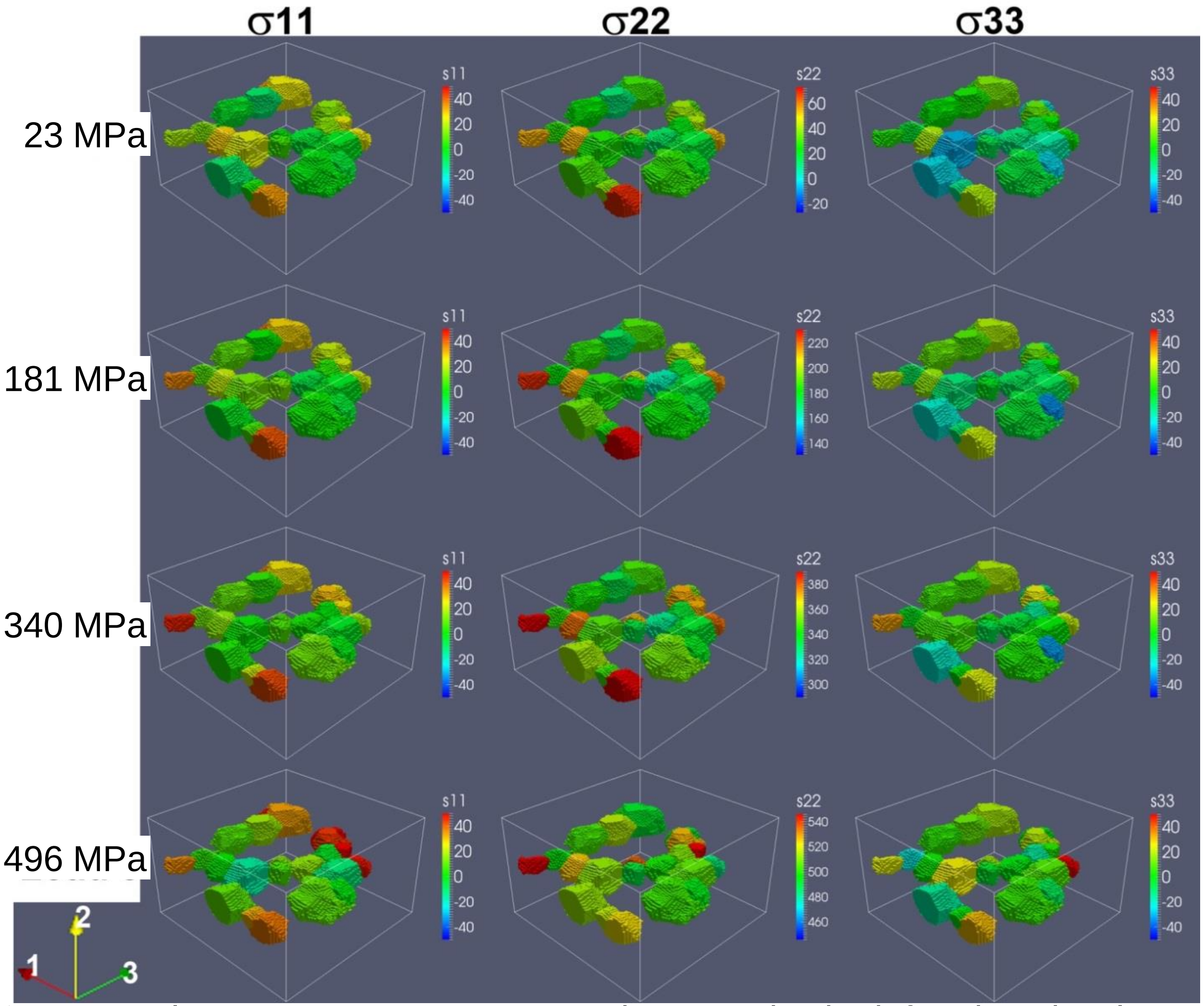

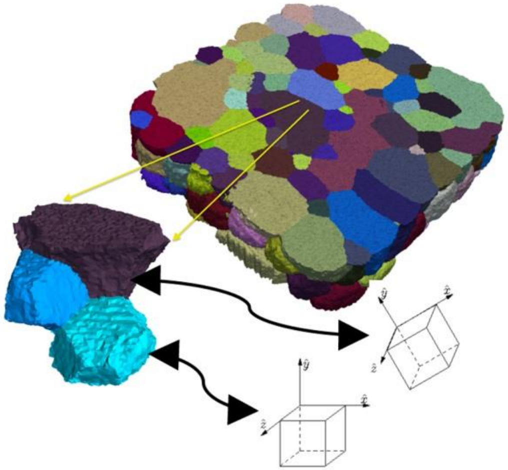

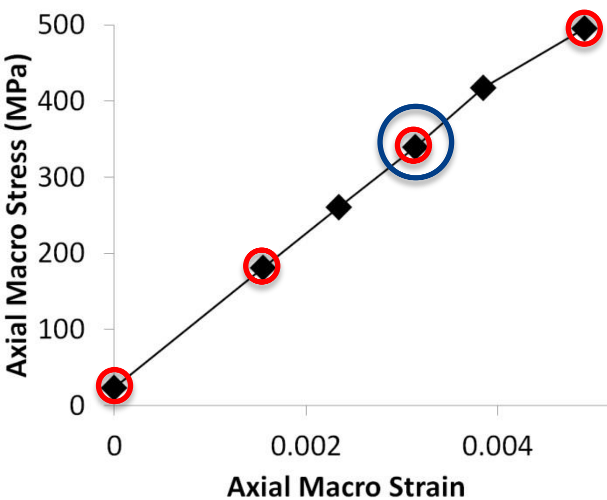

Shade PA, Blank B, Schuren JC, Turner TJ, Kenesei P, Goetze K, Suter RM, Bernier JV, Li SF, Lind J, Lienert U, Almer J. 2015. *Rev. Sci. Instrum.* 86:093902

- Normal stress components mapped onto grains in deforming Ti-7Al
- Shear components not shown to save space

Crack Initiation in Ni Superalloy with Seeded Inclusion

Ultrasonic Inspection of bulk RR1000 to determine regions with an inclusion

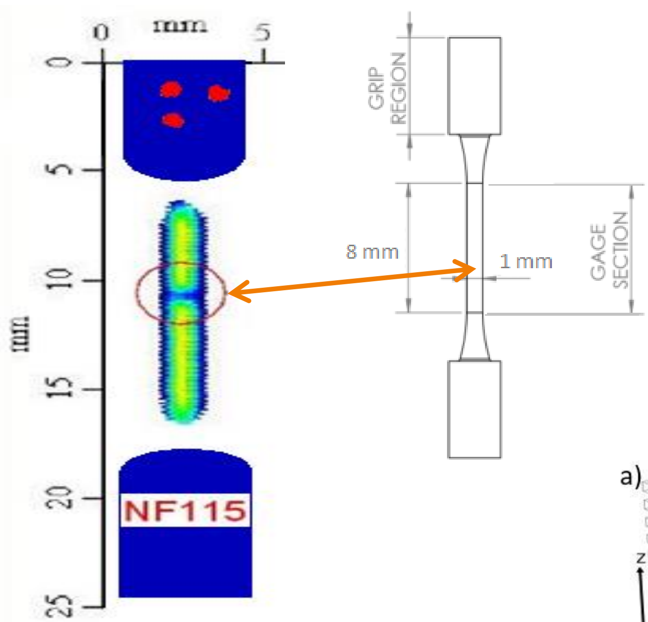

Naragani D, Sangid MD, Shade PA, Schuren JC, Sharma H, Park J-S, Kenesei P, Bernier JV, Turner TJ, Parr I. 2017. *Acta Mater.*

μ-CT Reconstruction

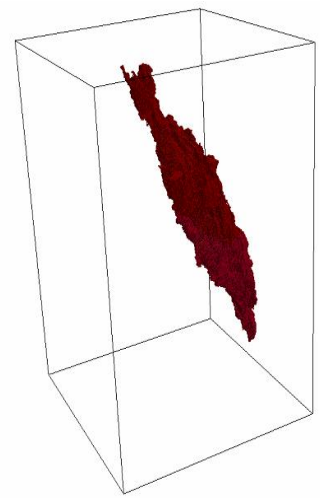

Integration of μ-CT and FF data

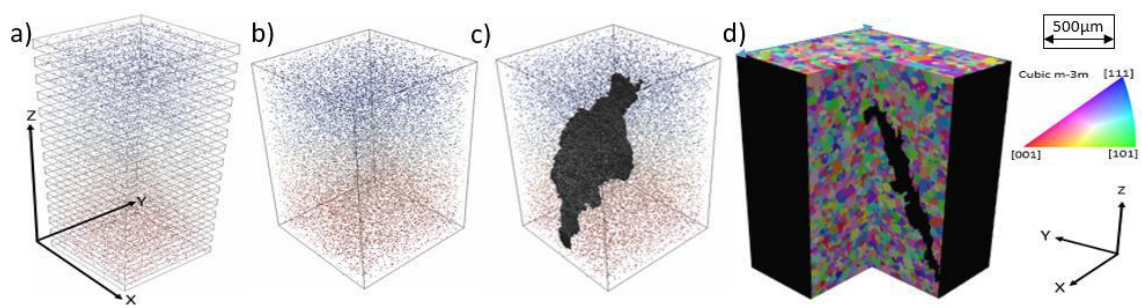

μ-CT and FF data (~40,000 grains in 15 layers) collected at 30 different loading steps (from 0 to 10,000 cycles)

Crack Initiation in Ni Superalloy with Seeded Inclusion

Crack observed after 10,000 loading cycles

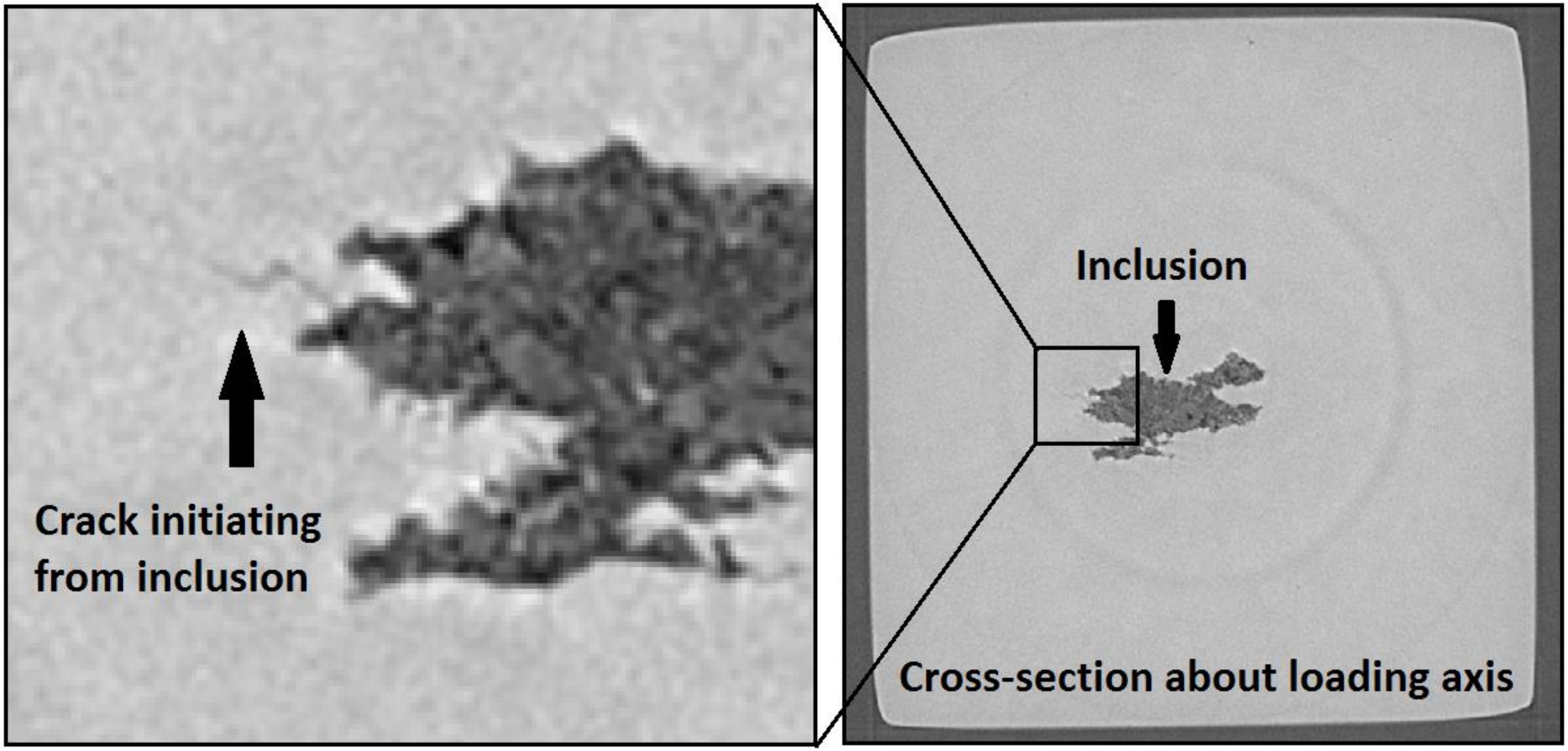

Naragani D, Sangid MD, Shade PA, Schuren JC, Sharma H, Park J-S, Kenesei P, Bernier JV, Turner TJ, Parr I. 2017. *Acta Mater.*

Crack Initiation in Ni Superalloy with Seeded Inclusion

Stress along tensile axis after 10,000 cycles

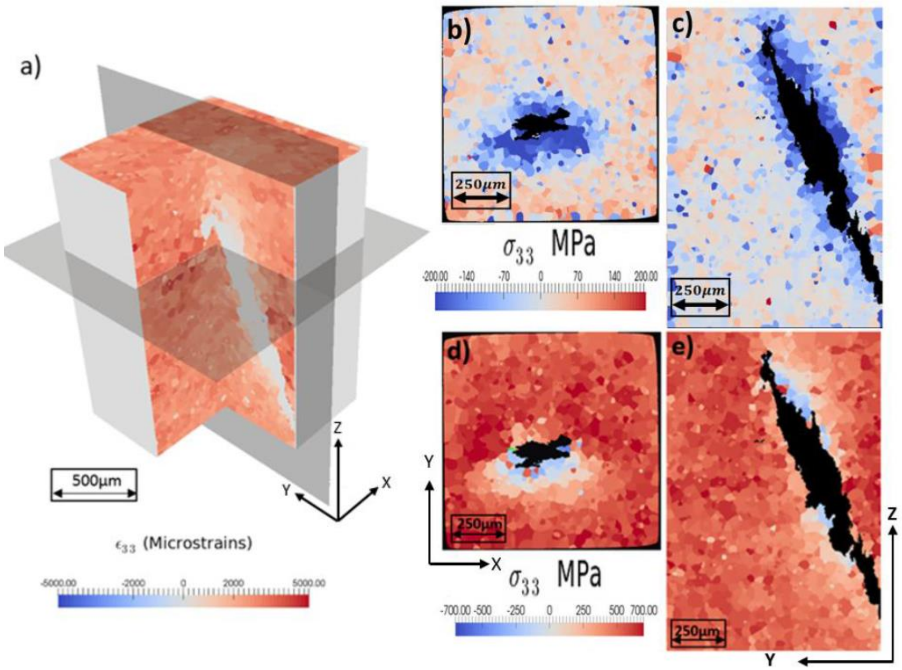

Stress gradients in qualitative agreement with experiment for simulation that includes residual stress and partial debonding

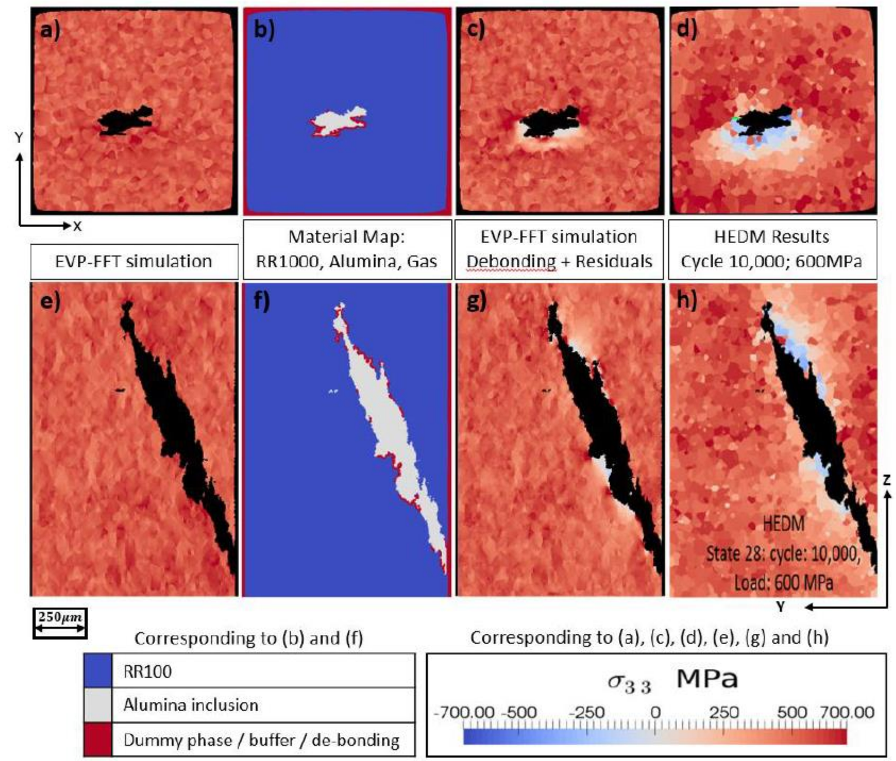

Naragani D, Sangid MD, Shade PA, Schuren JC, Sharma H, Park J-S, Kenesei P, Bernier JV, Turner TJ, Parr I. 2017. *Acta Mater.*

Partial debonding at matrix-inclusion interface shown to play pivotal role in creating stress gradient that led to crack initiation

MID^{3}AS Model Aggregation Vision

Synthetic phantoms for 'model of model' techniques

Sandia Fracture Challenge

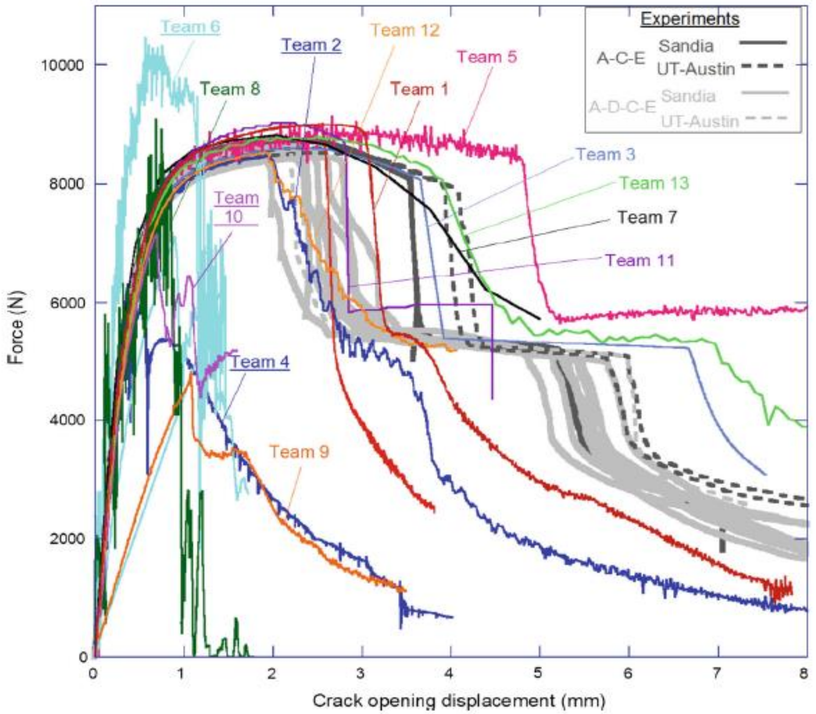

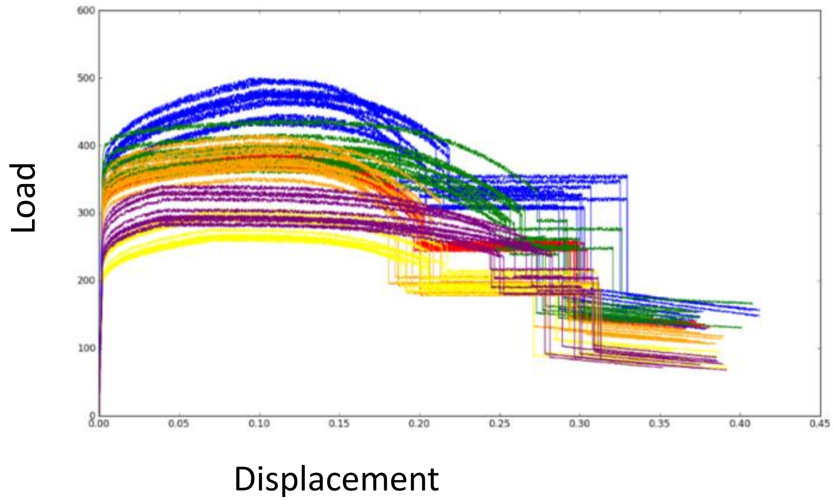

B.L. Boyce, et al. Int. J. Fracture. March 2014, **186**, 1–2. p5–68

Accounting for learned biases could tighten uncertainty in aggregate model

MID³AS Model Aggregation Vision

Modeling challenges should provide combinations of physics, implementation and input data, providing opportunity to learn biases to weight predictions in probabilistic framework.

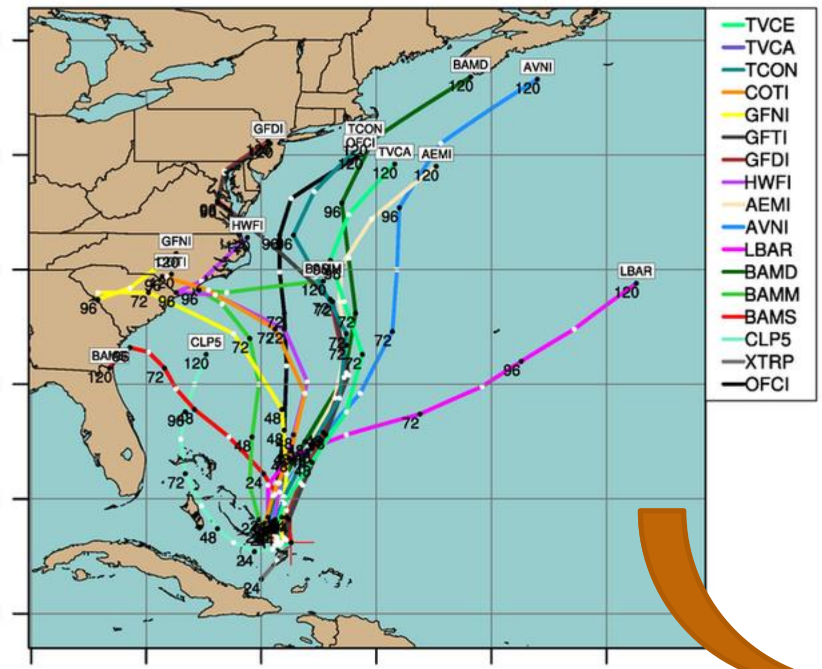

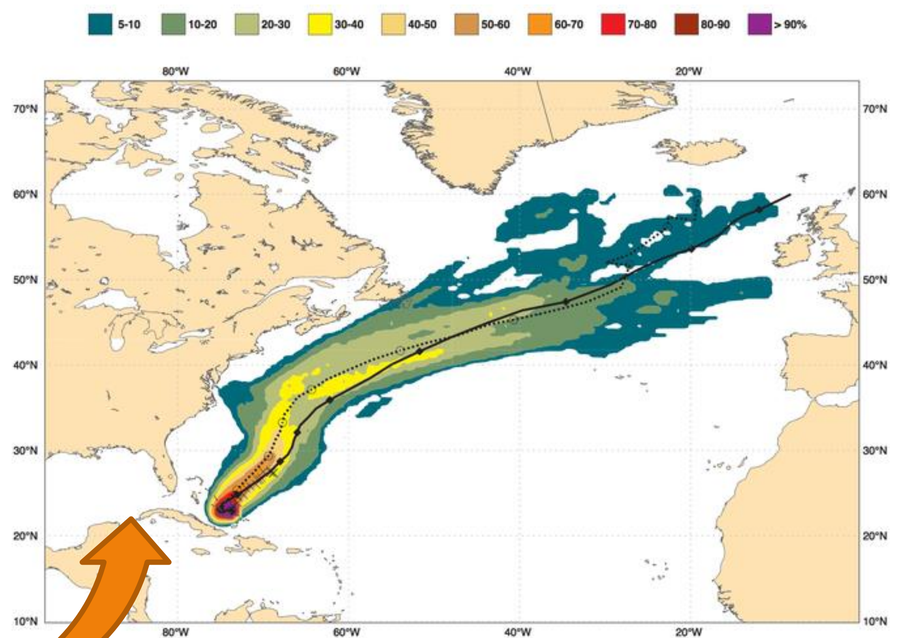

Weather community has shown multiple predictions improve forecasting fidelity